

Design and Optimization of a Large-Stroke Compliant Constant-Torque Mechanism

Thanh-Vu Phan, Huy-Tuan Pham *

HCMC University of Technology and Education, Vietnam

* Corresponding author. Email: phtuan@hcmute.edu.vn

ARTICLE INFO

Received: 18/12/2021
Revised: 26/1/2022
Accepted: 26/1/2022
Published: 28/2/2022

KEYWORDS

Constant-torque mechanism;
Compliant mechanism;
Genetic algorithm;
Finite element analysis;
Rotary mechanism.

ABSTRACT

Compliant constant-torque mechanism (CTM) can produce an output torque that does not change within a prescribed input rotation range. This stability is maintained regardless of complicated sensorized control systems. Owing to the monolithic nature of the compliant mechanism, the device is more compact, lightweight, and portable, which is favorable to human joint rehabilitative devices or mobility-assisting devices. However, before approaching the stable range, the mechanism has to undergo a pre-loading range which usually accounts for one-third of the entire operational journey. In addition, the deformation of flexible segments is restricted due to the yield strength of the materials. This limited working range hampers other potential applications of compliant CTMs. This paper presents a novel design of a compliant 2-stage CTM with long-stroke by using serially connected curved beams that deform sequentially. The design process is implemented via a shape optimization scheme using genetic algorithm. Finite element analysis is used to characterize the constant-torque behavior of the CTM under static loading. A general design formulation is also proposed to synthesize this special kind of compliant mechanism. The results show that this CTM gets the stable torque range from 30^0 to 110^0 over two stages with the deviation less than 4.3%.

Doi: <https://doi.org/10.54644/jte.68.2022.1098>

Copyright © JTE. This is an open access article distributed under the terms and conditions of the [Creative Commons Attribution-NonCommercial 4.0 International License](https://creativecommons.org/licenses/by-nc/4.0/) which permits unrestricted use, distribution, and reproduction in any medium for non-commercial purpose, provided the original work is properly cited.

1. Introduction

Unlike traditional rigid-body mechanisms, compliant mechanisms (CMs) are mechanical devices that achieve motion via elastic deformation of flexible segments. CMs take advantage of a monolithic structure including no backlash, no friction, no wear, no lubrication but still ease of fabrication [1]. Constant-torque mechanism (CTM) is a variant of constant-force mechanism (CFM) which has been attracting many researchers for decades [2-13]. CTMs generate an unchanged output torque regardless of the input rotation. Such mechanisms make the force control process become much simpler instead of using a complicated feedback system with actuators and sensors [14-17]. Hence, CTMs have plenty of potential applications in medical equipment such as mobility-assisting or rehabilitative devices, dynamic and static balancing of machines [18] as well as aerospace applications [19].

Compared to the blooming development of the counterpart CFMs during the last decades, compliant CTMs have just been noticing in recent years. Hou et al. designed a compliant CTM used as a functional joint mechanism [18]. Other compliant CTMs were synthesized by employing variable-width spline curves [20] or straight beams [21]. In our previous work [22], a novel design of a CTM for a rehabilitation device was developed by using Bezier curves. The major obstacle of all compliant CTMs during their trips to the operational range is that they have to undergo the preloading range which usually amounts to one-third of the total angular motion. In addition, the deformation of flexible members is restricted due to the yield strength of materials. This limited working range hampers other potential applications of compliant CTMs. In recent literature, this dilemma is eradicated by using pre-compressed beams as building blocks for compliant CTMs [23, 24]. Regardless of all these efforts, their absolute working ranges are still humble.

The concept of creating a CTM in this paper is to regulate the torque-rotation curve of a bi-stable mechanism to convert the negative stiffness region into a zero stiffness section. In order to further prolonging the working range of the CTM, this research proposes stacking two CTMs in a serial manner whilst maintaining the overall compactness of the device.

2. Design

2.1 Design concept and Operational principle

Instead of abiding by Hooke's law like conventional CMs, CTMs exhibit an irregular torque curve that radically differs from the purely elastic mechanism as shown in Fig. 1. After the pre-stress range, the mechanism approaches the quasi-zero stiffness in the constant-torque range. The output torque is stable irrespective of the variation of the input rotation. In this research, two stages of CTMs are serially connected which will lead to the sequential operation of each stage depending on their stiffness.

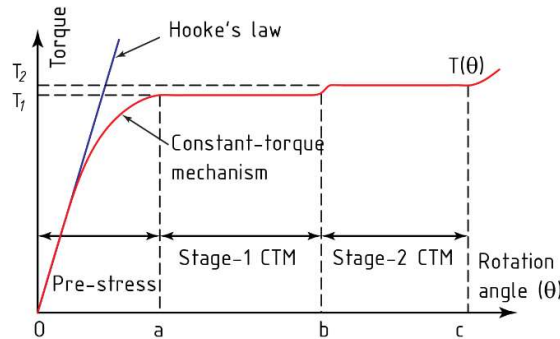


Fig. 1 - Torque – rotation curve of a stacked compliant CTM.

The schematic of a long-stroke CTM in this paper is proposed in Fig. 2. The idea of inducing a constant torque reaction while the CM deforms is to exploit the snap-through behavior of a specially designed curved beam as shown in Fig. 2(a). In this paper, Bezier curve is used to parameterize these beams. A reasonable circumferential arrangement of three alike beams will facilitate its axially symmetric deformation. In order to maintain the overall small size, two-stage CTMs with different stiffness are designed.

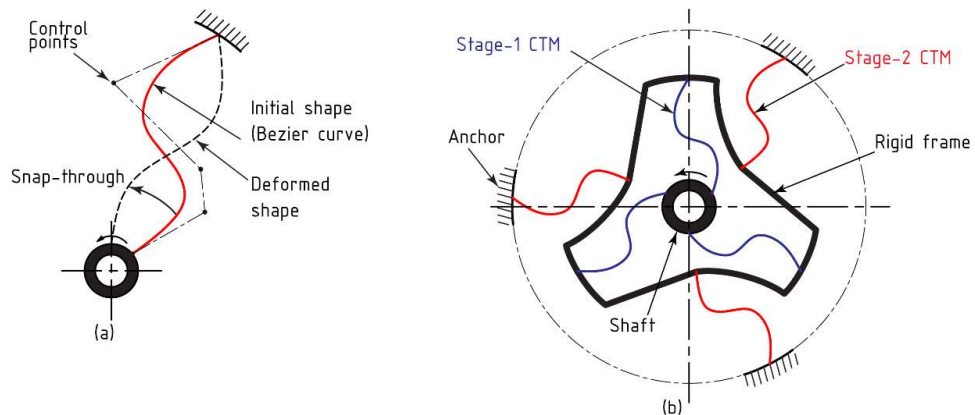


Fig. 2- Schematic design of a CTM (a) and its 2-stages long-stroke design concept (b).

In Fig. 2(b), three inner beams of the stage-1 CTM are mounted on a ring associated with a shaft providing the input rotation. Their other ends are linked to a rigid frame to transfer the rotational motion to three outer beams of the stage-2 CTM. These outer curved beams, which have fixed ends by the anchors, will continue deforming after receiving the motion.

2.2 Optimization design of the CTM.

Shape and size of the curves are obtained via an optimization of Genetic Algorithm (GA) carried out in MATLAB, and verified by means of finite element analysis (FEA) conducted in ABAQUS. To define the shape of Bezier curves, control points must be determined. Owing to the symmetry of the design, only one branch of each level illustrated as beam 1 and beam 2 is analyzed, shown in Fig. 3.

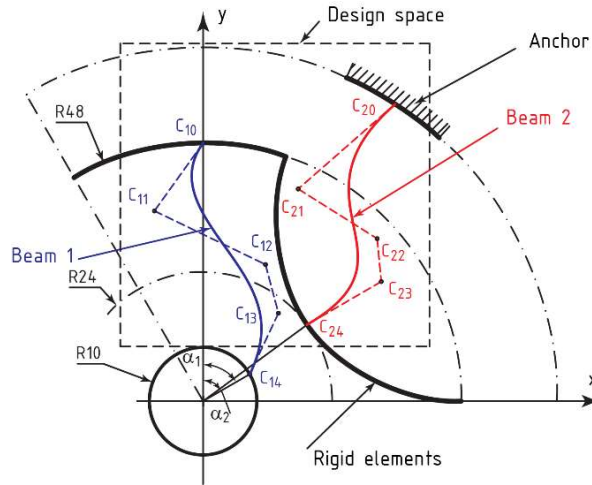


Fig. 3- Schematic of the design variables

For the sake of simplicity, fourth-order Bezier curve beams are chosen for the two beams. As a rule of thumb, the computer resources consumption is usually proportional to the number of design variables. Therefore some parameters of the CTM are constrained. Here, radii of the outer end of beam 1 and the inner end of beam 2 are predefined as R48 and R24, respectively. Radius of the center annular shape that attaches to point C_{14} is also a predefined parameter (R10) so that it could provide enough space to set up the shaft. The control point C_{10} is constrained to the vertical centerline and it is the intersection of this line with the circle R48. Therefore, there are totally 17 design variables including the (x, y) coordinates of $C_{11}, C_{12}, C_{13}, C_{20}, C_{21}, C_{22}, C_{23}$ and the angles (α_1, α_2) defining C_{14}, C_{24} , respectively, as well as a uniform width (w) of the beams.

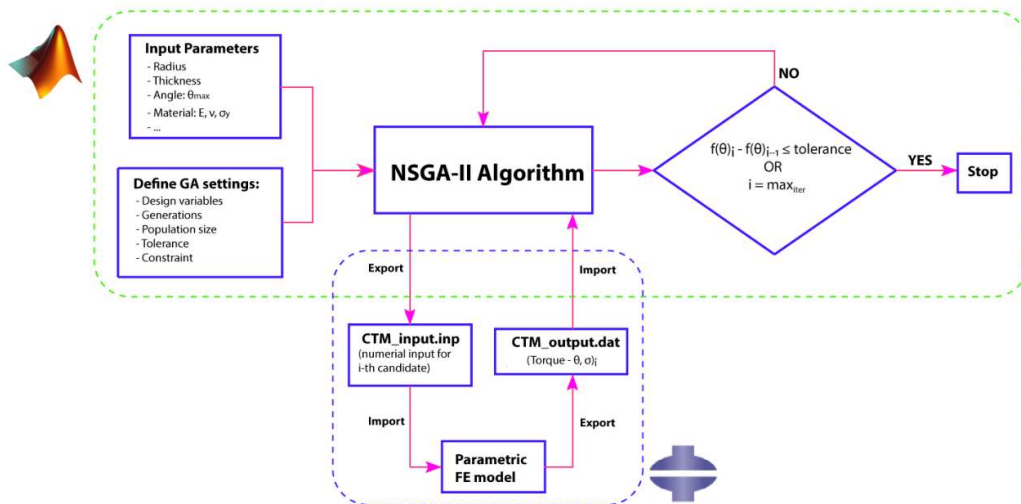


Fig. 4 - Flowchart of the FEA-based genetic algorithm optimization procedure

Trial designs are randomly created by using MATLAB based on the preliminary parameters. FEA by ABAQUS is applied to obtain the behavior between output torque and rotation angle. Simultaneously, the stress is also evaluated to assure the operation of the CTM within the elastic regime. To simulate precisely the relationship of flexible segments, the outer end of beam 1 (C_{10}) must rotate on the circle R48. Thus, FEA is applied for all six beams. The rigid links are replaced by 2-node beam elements for easier simulation. The flowchart of the GA which was verified to be suitable for solving constrained nonlinear problems is given in Fig. 4. The optimization was implemented automatically by MATLAB and ABAQUS. Inputs to the GA optimization are divided into two different boxes for the sake of better understanding of the algorithm. The “Input Parameters” and the “Define GA settings” boxes define the shape of the mechanism and the GA’s parameters, respectively. In the first loop, MATLAB produces the text codes “CTM_iput.txt” to define the simulation model based on the design parameters generated by GA. This model is then fed into the ABAQUS to implement the analysis. The torque – rotation curve is extracted from the simulation output file to evaluate the objective function in eq. (1). It is finally returned to the GA to calculate the fitness value for further sorting this design in the current generation. The nondominated-sorting genetic algorithm (NSGA-II) generates offspring using a specific type of crossover and mutation and then selects the next generation according to nondominated-sorting and crowding distance comparison. The algorithm is terminated when the objective function difference between two successive generations is smaller than the tolerance, the evolution is converged, or the initial number of generations (max_{iter}) is met. The optimization problem in this research is formulated in the following objective function:

$$\text{Min}[f(\theta)] = \int_a^b (T - T_1)^2 d\theta + \int_b^c (T - T_2)^2 d\theta \quad (1)$$

In eq. (1), a , b , and c are the margin between the pre-stress zone and the two working zones. The purpose of the objective function obtained in eq. (1) is to minimize the variation of the torque function $T(\theta)$ toward the two constant torques (T_1 and T_2) regardless the rotation angle of the mechanism in the working range. The numerical integration limits (a, b) and (b, c) depend on the configuration of the practical torque curve for each design. The criteria to choose these points is that $T(a)$, $T(b)$, and $T(c)$ should be within the tolerance of $\pm 5\%$ of T_1 and T_2 . Therefore, they are not predefined parameters of the optimization process. Generally, the optimization formulation is described in Table 1. To constraint the design space as well as to reduce the number of design variables, three radii are appropriately chosen for the purpose of CTM and prescribed as 10 mm, 24 mm, 48 mm, as shown in Fig. 3. Five constraint functions with different purposes are embedded to govern the optimization process. The functions g_1 and g_2 are to prevent the curved beams from intersecting each other. The functions g_3 and g_4 define the bound for the width of slender beams and the angles defining points C_{14} , C_{24} , respectively. The stress of the mechanism is required in the constraint g_5 .

Table 1. Formulation of a compliant constant torque mechanism optimization

1. Objective:
– Minimize the variation of the torque follow Eq. (1)
2. Design variables:
– Control points: $C_{ij}(x, y)$ ($i = 1 \div 2, j = 0 \div 4$)
– In-plane thickness: w
– Angles: α_1, α_2
3. Constraints:
i. $g_1: C_{11}(x) < 0;$
ii. $g_2: C_{1j}(x) > C_{2j}(x)$ ($j = 0 \div 4$)
iii. $g_3: 0.7 \leq w \leq 1.5$ (mm)
iv. $g_4: \pi/18 \leq \alpha \leq \pi/1.5$ (rad)
v. The maximum stress within the CTM, $g_5: \sigma_m < \sigma_y/SF$

3. Results and Discussion

The designed CTM suffers a large deformation, so choosing a proper material plays a vital role. In this model, PEEK (polyether etherketone) is selected because of the large ratio σ_y/E . This ratio is often used to measure the ability of a material to allow bending before yield. For the linear elastic and isotropic model, the Young's modulus (E) of PEEK is taken as 3.58 GPa, the Poisson's ratio (ν_p) is taken as 0.3, and the out-of-plane thickness of the structure is 5.0 mm.

Table 2. Optimum DVs of the CTM

Design variables	Values (mm)
$C_{10}(x, y)$	(0.00, 48.00)
$C_{11}(x, y)$	(-0.90, 25.47)
$C_{12}(x, y)$	(1.00, 32.53)
$C_{13}(x, y)$	(1.79, 32.53)
$C_{14}(x, y)$	(9.62, -2.74)
$C_{20}(x, y)$	(12.70, 58.13)
$C_{21}(x, y)$	(35.23, 58.13)
$C_{22}(x, y)$	(12.70, 35.60)
$C_{23}(x, y)$	(43.03, 15.90)
$C_{24}(x, y)$	(7.42, 22.83)
α_1	105.88°
α_2	18.00°
w	0.80

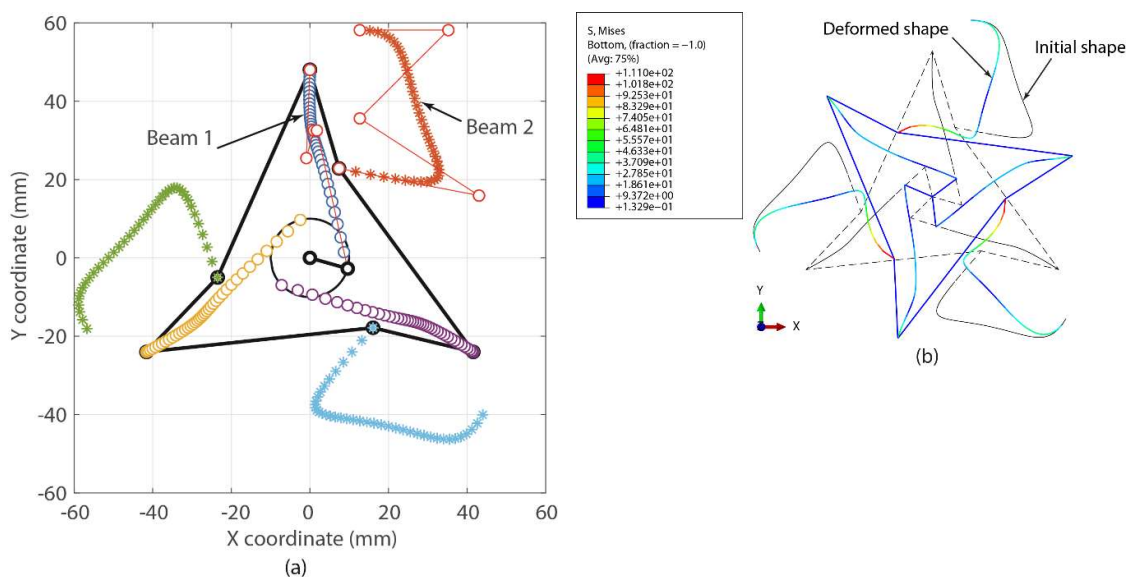


Fig. 5 - FEM beam element model (a) and simulation results (b)

The GA optimizations in MATLAB integrated with the FEA by ABAQUS are run with 30 generations and a population size of 40 candidates for each generation. The score is the optimal configurations of the proposed beam-based CTM shown in Fig. 5. These Bezier curved beams are created from the results of optimum design variables presented in Table 2. It is necessary to build a

three-dimension model to verify for the nonlinear stiffness and structural integrity of the mechanism and it is shown in Fig. 6. As seen in the Fig. 6, compliant members was structured in two floors to get enough space for the deformation to 110° . In the 3D simulation, the anchor ring was eliminated to reduce the computational time.

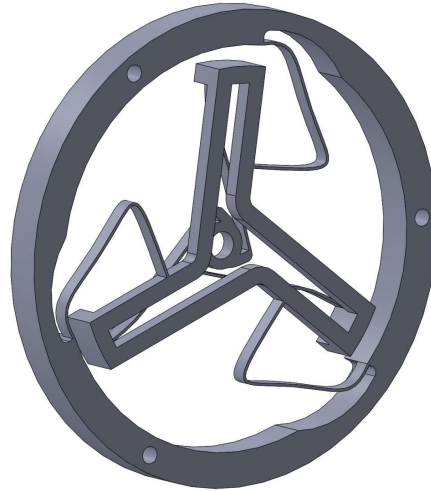


Fig. 6 - 3D model of the CTM

The torque – rotation curves of the optimum mechanism are indicated in Fig. 7. In this research, both beam element model (2D) and solid model (3D) are used to analyze the mechanical behavior of the mechanism. The former model is used during the optimization stage to fasten the evaluation of a design due to its simplicity. However, the tradeoff of this method is the approximated modelling to the real mechanism. It is advisable that the latter 3D-simulation should be implemented to verify the final results. Fig. 7 shows that the constant-torque value of 3D model is slightly higher than that of 2D model. But they are in good agreement of both cases. The constant-torque range is divided into two stages at the angle of 58° . The deviations of output torque of the CTM in the whole working range from 30° to 110° are 3.8% and 4.3% for 2D-beam model and 3D model, respectively, depicted in Table 3. The flatness of the torque curve between the operational ranges can be further improved by GA optimization algorithm if the generation evolution is extended. However, depending on the diversification of the initial population, global optimum solution in GA can also be hardly found if the whole generation are attracted to the local optima. The probability percentage of the two genetic operators in GA, crossover and mutation, can be intervened. Increasing the mutation possibility to produce more outsiders is one of the solutions to escape those local traps. In the current research, the variation of the torque between the working range is within the acceptable limits. Therefore, the evolution process is terminated after 30 generations. The torque can be adjusted to higher value by increasing the out-of-plane thickness without changing the flatness of the mechanism. The maximum stress of the mechanism stands at 128.6 MPa, shown in Fig. 7, is much smaller than the yield strength of the PEEK material ($\sigma_y = 210MPa$). The stack-up configuration of the CTM introduces more challenges for the conventional fabrication methods. However with the rapid advancement of 3D-printing technology, the manufacturing for such kind of products becomes much easier than ever. For PEEK material, several feasible printing methods are fused filament fabrication (FFF), stereolithography (SLA) or selective laser sintering (SLS). In 3D-printing technology, the accuracy for each method is evaluated by two criteria, namely, trueness and precision according to the ISO 5725-1:1994/COR 1:1998. Msallem et al. [25] showed that SLS has the highest trueness (0.11 ± 0.016 mm) when they printed the anatomical models for clinical application. This method will be used to print the current mechanism and will be presented in the next research.

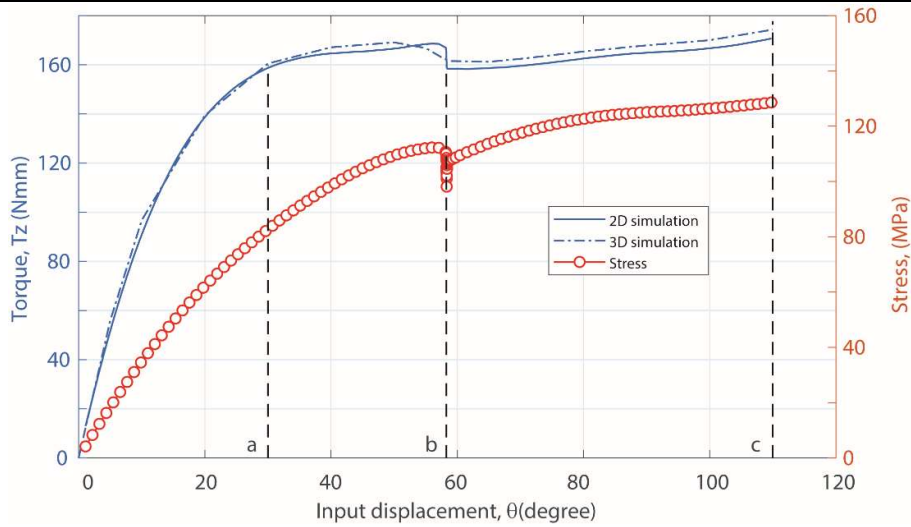


Fig. 7 - Torque and stress – rotation results using FEA analysis

Table 3. Output torque deviation

Model	Average value (at 40°)	Minimum (at 30°)	Maximum (at 110°)	Maximum Deviation (%)
2D	164.5	158.6	170.8	3.8
3D	167.1	160.5	174.3	4.3

3. Conclusions

In this paper, a simple and efficient method for the design of a compliant CTM was presented. A novel large-stroke CTM was proposed by using serially connected curved beams that deform sequentially. The optimum design is obtained by using genetic algorithm optimization coupled with finite element analysis. The enlarged operation range diversifies the probable applications for this kind of mechanism. In addition, taking the merits of compliant mechanisms, the designed CTM is a perfect replacement for the conventional mechatronic force control system, especially in mobility devices. In spite of the imperfect result, the proposed configuration is a worthy suggestion for extending the torque-constant range of other works in the future.

Acknowledgments

This work belongs to the project grant No: T2020-17 funded by Ho Chi Minh City University of Technology and Education, Vietnam.

REFERENCES

- [1] L. L. Howell, *Compliant mechanisms*. New York: Wiley, 2001.
- [2] X. Zhang and Q. Xu, "Design and analysis of a 2-DOF compliant gripper with constant-force flexure mechanism," *Journal of Micro-Bio Robotics*, vol. 15, no. 1, pp. 31-42, 2019.
- [3] X. Zhang and Q. Xu, "Design and testing of a novel 2-DOF compound constant-force parallel gripper," *Precision Engineering*, vol. 56, pp. 53-61, 2019.
- [4] X. Zhang and Q. Xu, "Design and development of a new 3-DOF active-type constant-force compliant parallel stage," *Mechanism and Machine Theory*, vol. 140, pp. 654-665, 2019.
- [5] Q. Xu, "Design of a large-stroke bistable mechanism for the application in constant-force micropositioning stage," *Journal of Mechanisms and Robotics*, vol. 9, p. 7, 2017.
- [6] G. W. Xiaozhi Zhang, Qingsong Xu "Design, Analysis and testing of a new compliant compound constant-force mechanism" *Actuators*, vol. 7, no. 4, 2018.
- [7] D.-A. Wang, J.-H. Chen, and H.-T. Pham, "A constant-force bistable micromechanism," *Sensors and Actuators A: Physical*, vol. 189, pp. 481-487, 2013.
- [8] C.-C. Lan, "A constant-force compliant gripper for handling objects of various sizes," *Journal of Mechanical Design*, vol. 136, p. 10, 2014.
- [9] H.-T. Pham and D.-A. Wang, "A constant-force bistable mechanism for force regulation and overload protection," *Mechanism and Machine Theory*, vol. 46, p. 11, 2011.

- [10] H.-T. Pham and N. H. N. Hieu, "Shape optimization and fabrication of a compliant constant - force mechanism," *Tap chí Khoa học và Công nghệ*, vol. 115, p. 6, 2016.
- [11] Y.-H. Chen and C.-C. Lan, "An adjustable constant-force mechanism for adaptive end-effector operations," *Journal of Mechanical Design*, vol. 134, no. 3, 2012.
- [12] P. Bilancia and G. Berselli, "Design and testing of a monolithic compliant constant force mechanism," *Smart Materials and Structures*, vol. 29, no. 4, p. 044001, 2020.
- [13] D. Nguyen, T.-V. Phan, and H.-T. Pham, "Design and analysis of a compliant gripper integrated with constant-force and static balanced mechanism for micro manipulation," in *2018 4th International Conference on Green Technology and Sustainable Development (GTSD)*, 2018, pp. 291-295.
- [14] R. R. Torrealba, S. B. Udelman, and E. D. Fonseca-Rojas, "Design of variable impedance actuator for knee joint of a portable human gait rehabilitation exoskeleton," *Mechanism and Machine Theory*, vol. 116, pp. 248-261, 2017.
- [15] Q. Liu et al., "Development of a new robotic ankle rehabilitation platform for hemiplegic patients after stroke," *Journal of Healthcare Engineering*, vol. 2018, 2018.
- [16] F. Sup, A. Bohara, and M. Goldfarb, "Design and control of a powered transfemoral prosthesis," *The International Journal of Robotics Research*, vol. 27, no. 2, pp. 263-273, 2008.
- [17] H. Aguilar-Sierra, W. Yu, S. Salazar, and R. Lopez, "Design and control of hybrid actuation lower limb exoskeleton," *Advances in Mechanical Engineering*, vol. 7, no. 6, 2015.
- [18] C.-W. Hou and C.-C. Lan, "Functional joint mechanisms with constant-torque outputs," *Mechanism and Machine Theory*, vol. 62, pp. 166-181, 2013/04/01/ 2013.
- [19] J. McGuire, "Analysis and design of constant-torque springs used in aerospace applications," PhD. Dissertation, The University of Texas at Austin, 1994.
- [20] H. Nair Prakashah and H. Zhou, "Synthesis of constant torque compliant mechanisms," *Journal of Mechanisms and Robotics*, vol. 8, no. 6, 2016.
- [21] P. Wang, S. Yang, and Q. Xu, "Design and optimization of a new compliant rotary positioning stage with constant output torque," *International Journal of Precision Engineering and Manufacturing*, vol. 19, no. 12, pp. 1843-1850, 2018/12/01 2018.
- [22] T.-V. Phan, and H.-T. Pham, and a. C.-N. Truong, "Design and analysis of a compliant constant-torque mechanism for rehabilitation devices," In: *Parinov L., Chang SH., Long B. (eds) Advanced Materials. Springer Proceedings in Materials*, vol. vol 6. Springer, Cham, p. 9, 2020.
- [23] I. Gandhi and H. Zhou, "Synthesizing constant torque compliant mechanisms using precompressed beams," *Journal of Mechanical Design*, vol. 141, no. 1, 2018.
- [24] P. Bilancia, S. P. Smith, G. Berselli, S. P. Magleby, and L. L. Howell, "Zero torque compliant mechanisms employing pre-buckled beams," *Journal of Mechanical Design*, vol. 142, no. 11, 2020.
- [25] Msallem, N. Sharma, S. Cao, F. S. Halbeisen, H.-F. Zeilhofer, and F. M. Thieringer, "Evaluation of the Dimensional Accuracy of 3D-Printed Anatomical Mandibular Models Using FFF, SLA, SLS, MJ, and BJ Printing Technology," *Journal of Clinical Medicine*, vol. 9, no. 3, 2020.



Thanh-Vu Phan received the M.S. degree in mechanical engineering from Ho Chi Minh City University of Technology and Education, Vietnam, in 2012. He is currently pursuing the Ph.D. degree in mechanical engineering at Ho Chi Minh City University of Technology and Education, Vietnam. His research interest includes compliant mechanisms and advanced manufacturing



Huy-Tuan Pham received the Ph.D. degree in precision engineering from National Chung Hsing University, Taiwan in 2011. He is currently an Associate Professor at Ho Chi Minh City University of Technology and Education, Vietnam. His research interest includes compliant mechanisms and their applications, ultrasonics and vibration-assisted machining methods.